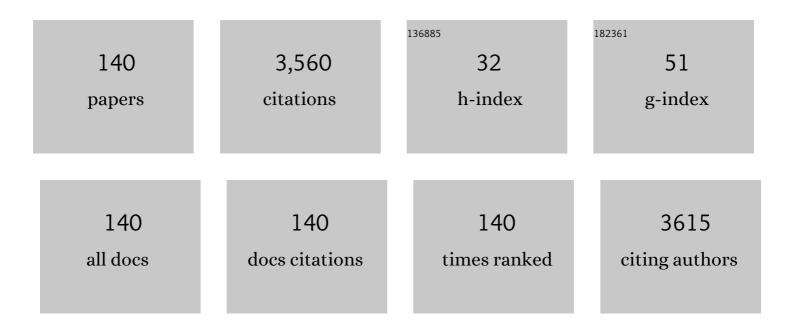
Jacob L Jaremko

List of Publications by Year in descending order

Source: https://exaly.com/author-pdf/150200/publications.pdf Version: 2024-02-01



#	Article	IF	CITATIONS
1	Blurring and Irregularity of the Subchondral Cortex in Pediatric Sacroiliac Joints on <scp>T1</scp> Images: Incidence of Normal Findings That Can Mimic Erosions. Arthritis Care and Research, 2023, 75, 190-197.	1.5	9
2	Discrete Choice Experiment on a Magnetic Resonance Imaging Scoring System for Temporomandibular Joints in Juvenile Idiopathic Arthritis. Arthritis Care and Research, 2022, 74, 308-316.	1.5	9
3	Health-Related Outcomes 3-15 Years Following Ankle Sprain Injury in Youth Sport: What Does the Future Hold?. Foot and Ankle International, 2022, 43, 21-31.	1.1	7
4	Metaphyseal and posterior rib fractures in osteogenesis imperfecta: Case report and review of the literature. Bone Reports, 2022, 16, 101171.	0.2	0
5	Improved-Mask R-CNN: Towards an accurate generic MSK MRI instance segmentation platform (data) Tj ETQq1	1 0,78431	4 rgBT /Over
6	Can Al Automatically Assess Scan Quality of Hip Ultrasound?. Applied Sciences (Switzerland), 2022, 12, 4072.	1.3	0
7	Concurrent validity and reliability of a semi-automated approach to measuring the magnetic resonance imaging morphology of the knee joint in active youth. Proceedings of the Institution of Mechanical Engineers, Part H: Journal of Engineering in Medicine, 2022, 236, 1023-1035.	1.0	1
8	Wrist Ultrasound Segmentation by Deep Learning. Lecture Notes in Computer Science, 2022, , 230-237.	1.0	4
9	Toward Developing a Semiquantitative Whole Body-MRI Scoring for Juvenile Idiopathic Arthritis: Critical Appraisal of the State of the Art, Challenges, and Opportunities. Academic Radiology, 2021, 28, 271-286.	1.3	14
10	Development of a technique for MRI gold-standard direct volumetric measurement of complex joint effusion, and validation at the hip. Skeletal Radiology, 2021, 50, 781-787.	1.2	1
11	MRI-based Synthetic CT in the Detection of Structural Lesions in Patients with Suspected Sacroiliitis: Comparison with MRI. Radiology, 2021, 298, 343-349.	3.6	80
12	Development and application of the average pelvic shape in virtual pelvic fracture reconstruction. International Journal of Medical Robotics and Computer Assisted Surgery, 2021, 17, e2199.	1.2	8
13	Normal subchondral high T2 signal on MRI mimicking sacroiliitis in children: frequency, age distribution, and relationship to skeletal maturity. European Radiology, 2021, 31, 3498-3507.	2.3	20
14	Quantitative analysis of regional specific pelvic symmetry. Medical and Biological Engineering and Computing, 2021, 59, 369-381.	1.6	2
15	Automated detection of pneumonia in lung ultrasound using deep video classification for COVID-19. Informatics in Medicine Unlocked, 2021, 25, 100687.	1.9	12
16	Impact of scan quality on AI assessment of hip dysplasia ultrasound. Journal of Ultrasound, 2021, , 1.	0.7	9
17	Diagnostic Accuracy of 3D Ultrasound and Artificial Intelligence for Detection of Pediatric Wrist Injuries. Children, 2021, 8, 431.	0.6	13
18	Volumetric quantitative measurement of hip effusions by manual versus automated artificial intelligence techniques: An OMERACT preliminary validation study. Seminars in Arthritis and Rheumatism, 2021, 51, 623-626.	1.6	6

#	Article	IF	CITATIONS
19	Artificial Intelligence to Automatically Assess Scan Quality in Hip Ultrasound. Indian Journal of Orthopaedics, 2021, 55, 1535-1542.	0.5	3
20	Arthritis and enthesitis in the hip and pelvis region in spondyloarthritis - OMERACT validation of two whole-body MRI methods. Seminars in Arthritis and Rheumatism, 2021, 51, 940-945.	1.6	6
21	Consensus-driven conceptual development of a standardized whole body-MRI scoring system for assessment of disease activity in juvenile idiopathic arthritis: MRI in JIA OMERACT working group. Seminars in Arthritis and Rheumatism, 2021, 51, 1350-1359.	1.6	15
22	The OMERACT Knee Inflammation MRI Scoring System: Validation of quantitative methodologies and tri-compartmental overlays in osteoarthritis. Seminars in Arthritis and Rheumatism, 2021, 51, 925-928.	1.6	4
23	Joint and entheseal inflammation in the knee region in spondyloarthritis - reliability and responsiveness of two OMERACT whole-body MRI scores. Seminars in Arthritis and Rheumatism, 2021, 51, 933-939.	1.6	4
24	Assessing the Reliability of the OMERACT Juvenile Idiopathic Arthritis Magnetic Resonance Scoring System for Temporomandibular Joints (JAMRIS-TMJ). Journal of Clinical Medicine, 2021, 10, 4047.	1.0	12
25	Magnetic resonance imaging findings in the normal pediatric sacroiliac joint space that can simulate disease. Pediatric Radiology, 2021, 51, 2530-2538.	1.1	4
26	Reliability of the Preliminary OMERACT Juvenile Idiopathic Arthritis MRI Score (OMERACT JAMRIS-SIJ). Journal of Clinical Medicine, 2021, 10, 4564.	1.0	6
27	Narrative Review on the Role of Imaging in DDH. Indian Journal of Orthopaedics, 2021, 55, 1456-1465.	0.5	7
28	Pediatric Imaging of the Elbow: A Pictorial Review. Seminars in Musculoskeletal Radiology, 2021, 25, 558-565.	0.4	0
29	MRI Knee Domain Translation for Unsupervised Segmentation By CycleGAN (data from Osteoarthritis) Tj ETQq1	1 0.78431	4 rgBT /Overl
30	Automatic Assessment Of Hip Effusion From MRI. , 2021, 2021, 3044-3048.		1
31	The Accuracy of Prevalent Vertebral Fracture Detection in Children Using Targeted Caseâ€Finding Approaches. Journal of Bone and Mineral Research, 2020, 35, 460-468.	3.1	8
32	Coronal Flexion Versus Coronal Neutral Sonographic Views in Infantile DDH: An Important Source of Variability. Journal of Pediatric Orthopaedics, 2020, 40, e440-e445.	0.6	2
33	Investigation of pelvic symmetry using CAD software. Medical and Biological Engineering and Computing, 2020, 58, 75-82.	1.6	16
34	Analysis of four methods of measuring three-dimensional pelvic tilt in the lateral decubitus position. Medical and Biological Engineering and Computing, 2020, 58, 2387-2396.	1.6	0
35	Diagnostic performance for erosion detection in sacroiliac joints on MR T1-weighted images: Comparison between different slice thicknesses. European Journal of Radiology, 2020, 133, 109352.	1.2	8
36	Imaging assessment of children presenting with suspected or known juvenile idiopathic arthritis: ESSR-ESPR points to consider. European Radiology, 2020, 30, 5237-5249.	2.3	39

#	Article	IF	CITATIONS
37	Toward an Improved Wrist View: Qualitative and Quantitative Investigation of the 20° Axial Lateral Wrist X-Ray. Journal of Medical Imaging and Radiation Sciences, 2020, 51, 280-288.	0.2	2
38	Normal hip joint fluid volumes in healthy children of different ages, based on MRI volumetric quantitative measurement. Pediatric Radiology, 2020, 50, 1587-1593.	1.1	2
39	Automated thyroid nodule detection from ultrasound imaging using deep convolutional neural networks. Computers in Biology and Medicine, 2020, 122, 103871.	3.9	59
40	Bone marrow edema in sacroiliitis: detection with dual-energy CT. European Radiology, 2020, 30, 3393-3400.	2.3	25
41	Low back pain and radiographic severity as predictors in hip osteoarthritis patients receiving steroid injection therapy. HIP International, 2020, 30, 187-194.	0.9	3
42	Virtual reconstruction of unilateral pelvic fractures by using pelvic symmetry. International Journal of Computer Assisted Radiology and Surgery, 2020, 15, 1267-1277.	1.7	15
43	The Accuracy of Incident Vertebral Fracture Detection in Children Using Targeted Case-Finding Approaches. Journal of Bone and Mineral Research, 2020, 36, 1255-1268.	3.1	3
44	A Validated Risk Prediction Model for Bone Fragility in Children With Acute Lymphoblastic Leukemia. Journal of Bone and Mineral Research, 2020, 36, 2290-2299.	3.1	5
45	MRI of the axial skeleton in spondyloarthritis: the many faces of new bone formation. Insights Into Imaging, 2019, 10, 67.	1.6	8
46	Ethics of Artificial Intelligence in Radiology: Summary of the Joint European and North American Multisociety Statement. Journal of the American College of Radiology, 2019, 16, 1516-1521.	0.9	48
47	Ethics of Artificial Intelligence in Radiology: Summary of the Joint European and North American Multisociety Statement. Canadian Association of Radiologists Journal, 2019, 70, 329-334.	1.1	81
48	Ethics of Artificial Intelligence in Radiology: Summary of the Joint European and North American Multisociety Statement. Radiology, 2019, 293, 436-440.	3.6	203
49	The OMERACT MRI in Enthesitis Initiative: Definitions of Key Pathologies, Suggested MRI Sequences, and a Novel Heel Enthesitis Scoring System. Journal of Rheumatology, 2019, 46, 1232-1238.	1.0	37
50	Hip Inflammatory Conditions: A Practical Differential Diagnosis Algorithmic Approach in Adults and Children. Seminars in Musculoskeletal Radiology, 2019, 23, e1-e16.	0.4	0
51	Diagnostic Accuracy of MRI-Based Sacroiliitis Scoring Systems: A Systematic Review. American Journal of Roentgenology, 2019, 212, 1112-1125.	1.0	11
52	Canadian Association of Radiologists White Paper on Ethical and Legal Issues Related to Artificial Intelligence in Radiology. Canadian Association of Radiologists Journal, 2019, 70, 107-118.	1.1	118
53	Preliminary Definitions for Sacroiliac Joint Pathologies in the OMERACT Juvenile Idiopathic Arthritis Magnetic Resonance Imaging Score (OMERACT JAMRIS-SIJ). Journal of Rheumatology, 2019, 46, 1192-1197.	1.0	23
54	OMERACT Hip Inflammation Magnetic Resonance Imaging Scoring System (HIMRISS) Assessment in Longitudinal Study. Journal of Rheumatology, 2019, 46, 1239-1242.	1.0	7

#	Article	IF	CITATIONS
55	Development and Validation of an OMERACT MRI Whole-Body Score for Inflammation in Peripheral Joints and Entheses in Inflammatory Arthritis (MRI-WIPE). Journal of Rheumatology, 2019, 46, 1215-1221.	1.0	35
56	Reliability of 2D and 3D ultrasound for infant hip dysplasia in the hands of novice users. European Radiology, 2019, 29, 1489-1495.	2.3	29
57	Health-related Outcomes after a Youth Sport–related Knee Injury. Medicine and Science in Sports and Exercise, 2019, 51, 255-263.	0.2	38
58	Prediction of mechanical behavior of cartilaginous infant hips in pavlik harness: A subjectâ€specific simulation study on normal and dysplastic hips. Journal of Orthopaedic Research, 2019, 37, 655-664.	1.2	4
59	Diagnostic ultrasound assessment of temporomandibular joints: a systematic review and meta-analysis. Dentomaxillofacial Radiology, 2019, 48, 20180144.	1.3	21
60	Ethics of artificial intelligence in radiology: summary of the joint European and North American multisociety statement. Insights Into Imaging, 2019, 10, 101.	1.6	61
61	Preliminary Definitions for Sacroiliac Joint Pathologies in the OMERACT Juvenile Idiopathic Arthritis MRI Score (OMERACT JAMRISâ€SIJ). FASEB Journal, 2019, 33, 453.8.	0.2	Ο
62	Developmental Hip Dysplasia Diagnosis at Three-dimensional US: A Multicenter Study. Radiology, 2018, 287, 1003-1015.	3.6	25
63	Canadian Association of Radiologists White Paper on Artificial Intelligence in Radiology. Canadian Association of Radiologists Journal, 2018, 69, 120-135.	1.1	349
64	6â€The consequences of knee joint injury in youth sport. , 2018, , .		0
65	Association between MRI-defined osteoarthritis, pain, function and strength 3–10 years following knee joint injury in youth sport. British Journal of Sports Medicine, 2018, 52, 934-939.	3.1	48
66	Hip Inflammation MRI Scoring System (HIMRISS) to predict response to hyaluronic acid injection in hip osteoarthritis. Joint Bone Spine, 2018, 85, 475-480.	0.8	17
67	New bone formation in the intervertebral joint space in spondyloarthritis: An MRI study. European Journal of Radiology, 2018, 109, 210-217.	1.2	4
68	Magnetic Resonance Imaging in Rheumatology. Magnetic Resonance Imaging Clinics of North America, 2018, 26, 599-613.	0.6	7
69	Bone Morbidity and Recovery in Children With Acute Lymphoblastic Leukemia: Results of a Six-Year Prospective Cohort Study. Journal of Bone and Mineral Research, 2018, 33, 1435-1443.	3.1	79
70	End-to-end detection-segmentation network with ROI convolution. , 2018, , .		13
71	Radiographs in screening for sacroiliitis in children: what is the value?. Arthritis Research and Therapy, 2018, 20, 141.	1.6	19
72	Feasibility and reliability of the Spondyloarthritis Research Consortium of Canada sacroiliac joint inflammation score in children. Arthritis Research and Therapy, 2018, 20, 56.	1.6	25

#	Article	lF	CITATIONS
73	Hip Joint Contact Pressure Distribution During Pavlik Harness Treatment of an Infant Hip: A Patient-Specific Finite Element Model. Journal of Biomechanical Engineering, 2018, 140, .	0.6	6
74	Segmentation-by-detection: A cascade network for volumetric medical image segmentation. , 2018, , .		23
75	Ultrasound-guided spinal stereotactic system for intraspinal implants. Journal of Neurosurgery: Spine, 2018, 29, 292-305.	0.9	18
76	Feasibility and Reliability of the Spondyloarthritis Research Consortium of Canada Sacroiliac Joint Structural Score in Children. Journal of Rheumatology, 2018, 45, 1411-1417.	1.0	22
77	Semiautomatic classification of acetabular shape from three-dimensional ultrasound for diagnosis of infant hip dysplasia using geometric features. International Journal of Computer Assisted Radiology and Surgery, 2017, 12, 439-447.	1.7	11
78	Three-dimensional morphological changes of the temporomandibular joint and functional effects after mandibulotomy. Journal of Otolaryngology - Head and Neck Surgery, 2017, 46, 8.	0.9	10
79	Preliminary validation of the Knee Inflammation MRI Scoring System (KIMRISS) for grading bone marrow lesions in osteoarthritis of the knee: data from the Osteoarthritis Initiative. RMD Open, 2017, 3, e000355.	1.8	24
80	Validation of a Knowledge Transfer Tool for the Knee Inflammation MRI Scoring System for Bone Marrow Lesions According to the OMERACT Filter: Data from the Osteoarthritis Initiative. Journal of Rheumatology, 2017, 44, 1718-1722.	1.0	9
81	MRI-based hip cartilage measures in osteoarthritic and non-osteoarthritic individuals: a systematic review. RMD Open, 2017, 3, e000358.	1.8	4
82	Update on Pediatric Hip Imaging. Seminars in Musculoskeletal Radiology, 2017, 21, 561-581.	0.4	8
83	Validation of a Knowledge Transfer Tool According to the OMERACT Filter: Does Web-based Real-time Iterative Calibration Enhance the Evaluation of Bone Marrow Lesions in Hip Osteoarthritis?. Journal of Rheumatology, 2017, 44, 1713-1717.	1.0	8
84	Toward automatic diagnosis of hip dysplasia from 2D ultrasound. , 2017, , .		11
85	Usefulness of MRI-CBCT image registration in the evaluation of temporomandibular joint internal derangement by novice examiners. Oral Surgery, Oral Medicine, Oral Pathology and Oral Radiology, 2017, 123, 249-256.	0.2	15
86	Finite element analysis of mechanical behavior of human dysplastic hip joints: a systematic review. Osteoarthritis and Cartilage, 2017, 25, 438-447.	0.6	29
87	Multi-dimensional low rank plus sparse decomposition for reconstruction of under-sampled dynamic MRI. Pattern Recognition, 2017, 63, 667-679.	5.1	43
88	Three-Dimensional Assessment of Temporomandibular Joint Using MRI-CBCT Image Registration. PLoS ONE, 2017, 12, e0169555.	1.1	16
89	Normal Values and Variation of Radiographic and CT Infant Lateral Iliac Wall Angles in Normal and Dysplastic Hips. HIP International, 2016, 26, 602-607.	0.9	2
90	Effects of inter-individual lumbar spine geometry variation on load-sharing: Geometrically personalized Finite Element study. Journal of Biomechanics, 2016, 49, 2909-2917.	0.9	41

Jacob L Jaremko

#	Article	IF	CITATIONS
91	A Validation Study of a Novel 3-Dimensional MRI Modeling Technique to Identify the Anatomic Insertions of the Anterior Cruciate Ligament. Orthopaedic Journal of Sports Medicine, 2016, 4, 232596711667379.	0.8	7
92	Dynamic MRI reconstruction using low rank plus sparse tensor decomposition. , 2016, , .		10
93	Cross-Modality Validation of Acetabular Surface Models Using 3-D Ultrasound Versus Magnetic Resonance Imaging in Normal and Dysplastic Infant Hips. Ultrasound in Medicine and Biology, 2016, 42, 2308-2314.	0.7	8
94	Toward automated classification of acetabular shape in ultrasound for diagnosis of DDH: Contour alpha angle and the rounding index. Computer Methods and Programs in Biomedicine, 2016, 129, 89-98.	2.6	26
95	MRI and CBCT image registration of temporomandibular joint: a systematic review. Journal of Otolaryngology - Head and Neck Surgery, 2016, 45, 30.	0.9	53
96	Development of Image Overlay and Knowledge Transfer Module Technologies Aimed at Enhancing Feasibility and External Validation of Magnetic Resonance Imaging-based Scoring Systems. Journal of Rheumatology, 2016, 43, 223-231.	1.0	7
97	MRI alone versus MRI-CBCT registered images to evaluate temporomandibular joint internal derangement. Oral Surgery, Oral Medicine, Oral Pathology and Oral Radiology, 2016, 122, 638-645.	0.2	12
98	Magnetic Resonance Imaging in Patients with Mechanical Low Back Pain Using a Novel Rapid-Acquisition Three-Dimensional SPACE Sequence at 1.5-T: A Pilot Study Comparing Lumbar Stenosis Assessment with Routine Two-Dimensional Magnetic Resonance Sequences. Canadian Association of Radiologists Journal, 2016, 67, 368-378.	1.1	6
99	Radiographic sclerotic contour loss in the identification of glenoid bone loss. Knee Surgery, Sports Traumatology, Arthroscopy, 2016, 24, 2167-2173.	2.3	2
100	Accuracy of magnetic resonance imaging–cone beam computed tomography rigid registration of the head: an in-vitro study. Oral Surgery, Oral Medicine, Oral Pathology and Oral Radiology, 2016, 121, 316-321.	0.2	12
101	The Radiology of Vertebral Fractures in Childhood Osteoporosis Related to Glucocorticoid Administration. Journal of Clinical Densitometry, 2016, 19, 81-88.	0.5	16
102	An index for diagnosing infant hip dysplasia using 3-D ultrasound: the acetabular contact angle. Pediatric Radiology, 2016, 46, 1023-1031.	1.1	18
103	A technique for semiautomatic segmentation of echogenic structures in 3D ultrasound, applied to infant hip dysplasia. International Journal of Computer Assisted Radiology and Surgery, 2016, 11, 31-42.	1.7	30
104	Development and Preliminary Validation of a Digital Overlay-based Learning Module for Semiquantitative Evaluation of Magnetic Resonance Imaging Lesions in Osteoarthritis of the Hip. Journal of Rheumatology, 2016, 43, 232-238.	1.0	14
105	On the load-sharing along the ligamentous lumbosacral spine in flexed and extended postures: Finite element study. Journal of Biomechanics, 2016, 49, 974-982.	0.9	52
106	Diagnostic Value of MRI of the Sacroiliac Joints in Juvenile Spondyloarthritis. Journal of the Belgian Society of Radiology, 2016, 100, 95.	0.2	6
107	Incident Vertebral Fractures and Risk Factors in the First Three Years Following Glucocorticoid Initiation Among Pediatric Patients With Rheumatic Disorders. Journal of Bone and Mineral Research, 2015, 30, 1667-1675.	3.1	94
108	Common normal variants of pediatric vertebral development that mimic fractures: a pictorial review from a national longitudinal bone health study. Pediatric Radiology, 2015, 45, 593-605.	1.1	49

#	Article	IF	CITATIONS
109	Incident Vertebral Fractures in Children With Leukemia During the Four Years Following Diagnosis. Journal of Clinical Endocrinology and Metabolism, 2015, 100, 3408-3417.	1.8	93
110	Reproducibility of Acetabular Landmarks and a Standardized Coordinate System Obtained from 3D Hip Ultrasound. Ultrasonic Imaging, 2015, 37, 267-276.	1.4	13
111	Ultrasound Quantification of Acetabular Rounding in Hip Dysplasia: Reliability and Correlation to Treatment Decisions in a Retrospective Study. Ultrasound in Medicine and Biology, 2015, 41, 56-63.	0.7	7
112	Reliability of 3D localisation of ACL attachments on MRI: comparison using multi-planar 2D versus high-resolution 3D base sequences. Knee Surgery, Sports Traumatology, Arthroscopy, 2015, 23, 1206-1214.	2.3	14
113	Real-Time Visualization of Joint Cavitation. PLoS ONE, 2015, 10, e0119470.	1.1	46
114	Methodologies for Semiquantitative Evaluation of Hip Osteoarthritis by Magnetic Resonance Imaging: Approaches Based on the Whole Organ and Focused on Active Lesions. Journal of Rheumatology, 2014, 41, 359-369.	1.0	26
115	Reliability of Indices Measured on Infant Hip MRI at Time of Spica Cast Application for Dysplasia. HIP International, 2014, 24, 405-416.	0.9	22
116	Potential for Change in US Diagnosis of Hip Dysplasia Solely Caused by Changes in Probe Orientation: Patterns of Alpha-angle Variation Revealed by Using Three-dimensional US. Radiology, 2014, 273, 870-878.	3.6	59
117	Novel imaging modalities in spondyloarthritis. Best Practice and Research in Clinical Rheumatology, 2014, 28, 729-745.	1.4	2
118	MRI Anatomy of the Tibial ACL Attachment and Proximal Epiphysis in a Large Population of Skeletally Immature Knees. American Journal of Sports Medicine, 2014, 42, 1644-1651.	1.9	19
119	Meniscal Injury After Adolescent Anterior Cruciate Ligament Injury: How Long Are Patients at Risk?. Clinical Orthopaedics and Related Research, 2014, 472, 990-997.	0.7	63
120	MRI of the SI joints commonly shows non-inflammatory disease in patients clinically suspected of sacroiliitis. European Journal of Radiology, 2014, 83, 179-184.	1.2	53
121	Development and reliability of a multi-modality scoring system for evaluation of disease progression in pre-clinical models of osteoarthritis: celecoxib may possess disease-modifying properties. Osteoarthritis and Cartilage, 2014, 22, 1639-1650.	0.6	37
122	Doppler Ultrasound Velocities and Resistive Indexes Immediately After Pediatric Liver Transplantation: Normal Ranges and Predictors of Failure. American Journal of Roentgenology, 2014, 203, W110-W116.	1.0	28
123	Diagnostic Utility of Magnetic Resonance Imaging and Radiography in Juvenile Spondyloarthritis: Evaluation of the Sacroiliac Joints in Controls and Affected Subjects. Journal of Rheumatology, 2014, 41, 963-970.	1.0	60
124	Preliminary Validation of 2 Magnetic Resonance Image Scoring Systems for Osteoarthritis of the Hip According to the OMERACT Filter. Journal of Rheumatology, 2014, 41, 370-378.	1.0	29
125	Spectrum of injuries associated with paediatric ACL tears: an MRI pictorial review. Insights Into Imaging, 2013, 4, 273-285.	1.6	12
126	How specific is the MRI appearance of supratentorial atypical teratoid rhabdoid tumors?. Pediatric Radiology, 2013, 43, 347-354.	1.1	25

#	Article	IF	CITATIONS
127	Advanced Imaging of the Axial Skeleton in Spondyloarthropathy: Techniques, Interpretation, and Utility. Seminars in Musculoskeletal Radiology, 2012, 16, 389-400.	0.4	13
128	MR imaging findings and MR criteria for instability in osteochondritis dissecans of the elbow in children. European Journal of Radiology, 2012, 81, 1306-1310.	1.2	56
129	Whole-body MRI in neurofibromatosis: incidental findings and prevalence of scoliosis. Skeletal Radiology, 2012, 41, 917-923.	1.2	28
130	Incidence and Significance of Inconclusive Results in Ultrasound for Appendicitis in Children and Teenagers. Canadian Association of Radiologists Journal, 2011, 62, 197-202.	1.1	28
131	Patterns of complications of neonatal and infant meningitis on MRI by organism: A 10 year review. European Journal of Radiology, 2011, 80, 821-827.	1.2	34
132	Radiographic Assessment of Bone Remodelling inSlippedUpper Femoral Epiphyses Using Klein's Lineandthe α Angle of Femoral-Acetabular Impingement. Journal of Pediatric Orthopaedics, 2011, 31, 153-158.	0.6	25
133	MRI differentiates femoral condylar ossification evolution from osteochondritis dissecans. A new sign. European Radiology, 2011, 21, 1170-1179.	2.3	34
134	Evolution of Femoral Condylar Ossification at MR Imaging: Frequency and Patient Age Distribution. Radiology, 2011, 258, 880-888.	3.6	52
135	Accuracy and reliability of MRI vs. laboratory measurements in an ex vivo porcine model of arthritic cartilage loss. Journal of Magnetic Resonance Imaging, 2007, 26, 992-1000.	1.9	6
136	Reliability of an efficient MRI-based method for estimation of knee cartilage volume using surface registration. Osteoarthritis and Cartilage, 2006, 14, 914-922.	0.6	33
137	Comparison of Cobb Angles Measured Manually, Calculated from 3-D Spinal Reconstruction, and Estimated from Torso Asymmetry. Computer Methods in Biomechanics and Biomedical Engineering, 2002, 5, 277-281.	0.9	14
138	Genetic Algorithm–Neural Network Estimation of Cobb Angle from Torso Asymmetry in Scoliosis. Journal of Biomechanical Engineering, 2002, 124, 496-503.	0.6	31
139	Indices of torso asymmetry related to spinal deformity in scoliosis. Clinical Biomechanics, 2002, 17, 559-568.	0.5	54
140	Estimation of Spinal Deformity in Scoliosis From Torso Surface Cross Sections. Spine, 2001, 26, 1583-1591.	1.0	50